GSSI A.P. XXXII cycle

Multiple detector analysis in the CRESST Dark Matter experiment

PhD Candidate:
Stefano Di Lorenzo

Advisors:
Paolo Gorla INFN - LNGS
Carlo Bucci INFN - LNGS

16 October 2020

Outline

- The Quest for Dark Matter
- The CRESST experiment for Direct Dark Matter search
- Likelihood: a paradigm shift fot the CRESST analysis
- The Data Analysis workflow
- Physics Results

The Quest for Dark Matter

Evidence for Dark Matter

- Galactic rotation curve
- Bullet Cluster
- Structure formation
- Cosmic Microwave Background anisotropies
- ...

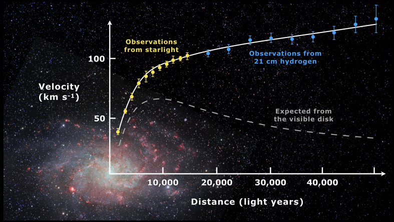

https://doi.org/10.1046/j.1365-8711.2000.03075.x

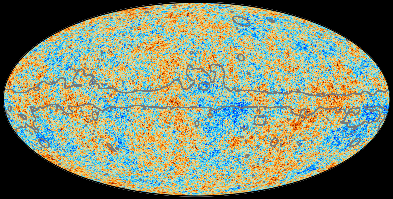

https://doi.org/10.1051/0004-6361/201936386

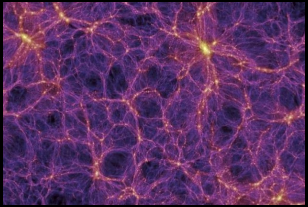

https://wwwmpa.mpa-garching.mpg.de/galform/virgo/millennium/

https://chandra.harvard.edu/photo/2006/1e0657/more.html

Dark Matter Abundance

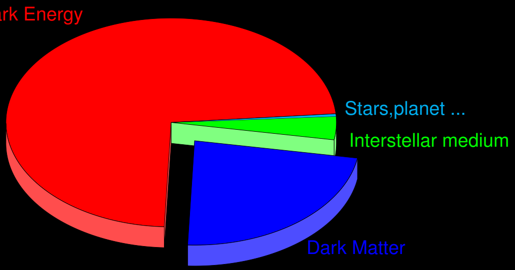

- Dark Energy 68.5%
- Dark Matter 26.5%
- Interstellar medium 4.6%
- Stars, planets, etc. 0.4%

Planck Mission
https://doi.org/10.1051/0004-6361/201833910

Dark Matter properties

- Gravitational interaction
- Stable or Long Lifetime
- Chargeless
- Cold i.e. non relativistic
- Local average density ($\sim$0.3 GeV/c^2cm^3)
- Total average density ($\sim$1 GeV/c^2m^3)
- Sub-weak interaction (??)

Candidates

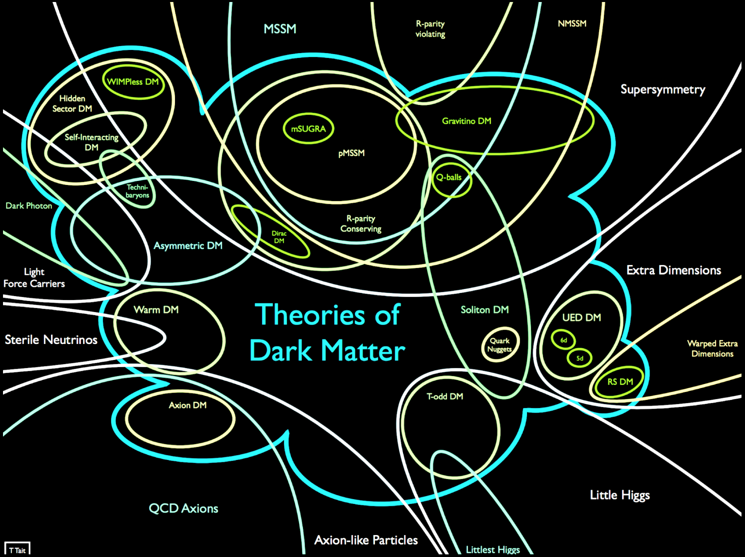

https://indico.cern.ch/event/473000/contributions/1993414/attachments/1209863/1764345/tait-Aspen.pdf

Experimental approaches

DM particles are naturally produced during interaction of particles beams

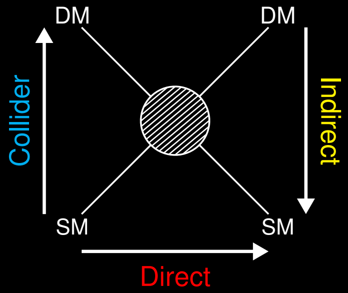

Annihilation or decay products of DM particles result in detectable species, especially gamma rays, neutrinos and antimatter particles

DM particles interact weakly via elastic and inelastic scattering with atomic nuclei or with electrons in the detector material

Dark Matter Halo

The Halo Model is a crucial aspect for the Dark Matter search.

Standard Halo Model

Spherical halo with Maxwell-Boltzmann velocity distribution truncated at the escape velocity of the galaxy $\sim$550 km/s [1]

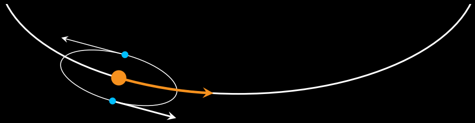

Key signature:
Annual modulation

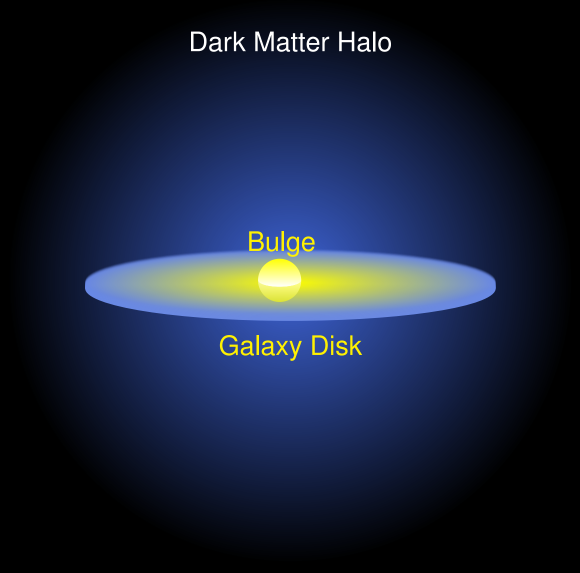

[1] https://iopscience.iop.org/article/10.1088/0004-637X/794/1/59f

Dark Matter Expected Spin-Independent Rate

$$\frac{dR}{dE_R dM} = n_\chi N_T \int_{v > v_{min}} v\, f(\vec{v}, \vec{v}_\oplus)\, \frac{d\sigma}{dE_R}\, d^3 v$$

$$n_\chi = \frac{\rho_\chi}{m_\chi}$$

$$v_{min} = \sqrt{\frac{E_{th} m_N}{2\mu^2}}$$

$$\frac{d\sigma}{dE_R} = \frac{\sigma_n}{v^2}\frac{m_N}{2\mu_n^2}\frac{[Zf_p + (A-Z)f_n]^2}{f_n^2} F^2(E_R)$$

$$\Downarrow\; f_n = f_p$$

$$\frac{d\sigma}{dE_R} = \frac{\sigma_n}{v^2}\frac{m_N}{2\mu_n^2} A^2 F^2(E_R)$$

Astro physics input

Nuclear physics input

Dark Matter Expected Spin-Independent Rate

$$\frac{dR}{dE_R dM} = n_\chi N_T \int_{v > v_{min}} v\, f(\vec{v}, \vec{v}_\oplus)\, \frac{d\sigma}{dE_R}\, d^3 v$$

Experimental Setup
N_t = number of target
A = Nucleus atomic mass
E_{th} = Energy threshold

$$n_\chi = \frac{\rho_\chi}{m_\chi} \qquad v_{min} = \sqrt{\frac{E_{th} m_N}{2\mu^2}}$$

$$\frac{d\sigma}{dE_R} = \frac{\sigma_n}{v^2}\frac{m_N}{2\mu_n^2}\frac{[Zf_p + (A-Z)f_n]^2}{f_n^2} F^2(E_R)$$

$$\Downarrow \; f_n = f_p$$

$$\frac{d\sigma}{dE_R} = \frac{\sigma_n}{v^2}\frac{m_N}{2\mu_n^2} A^2 F^2(E_R)$$

Astro physics input
Nuclear physics input

Target and Threshold effect on Rate

Since the cross section is $\propto A^2$, heavy nuclei, i.e. tungsten, have a large interaction rate.

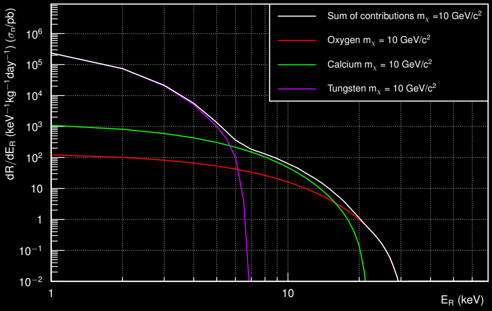

On the other hand the presence of an energy threshold favours light nuclei to explore the low mass region.

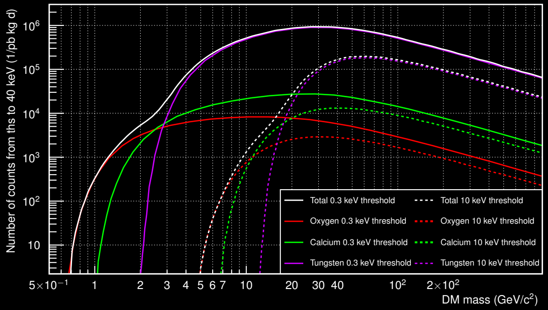

Direct search approach

- Double Phase TPC with Xenon (Xenon1T, LUX, Panda-X) or Argon (DarkSide)
- Room temperature NaI scintillating crystal (DAMA/LIBRA, COSINE-100, SABRE)
- Cryogenic detector (SuperCDMS, EDELWEISS, COSINUS, CRESST)
- Spherical proportional counter (NEWS-G)
- Directional detectors (NEWSdm, CYGNUS)

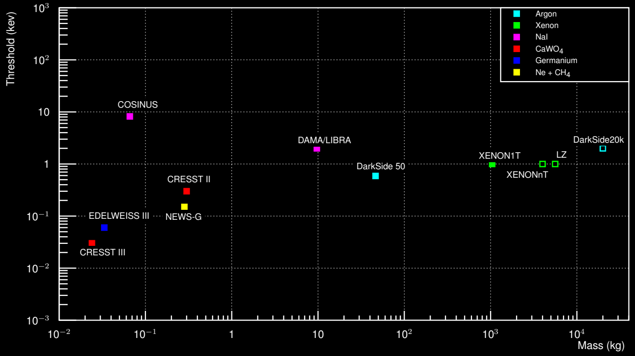

State of the art

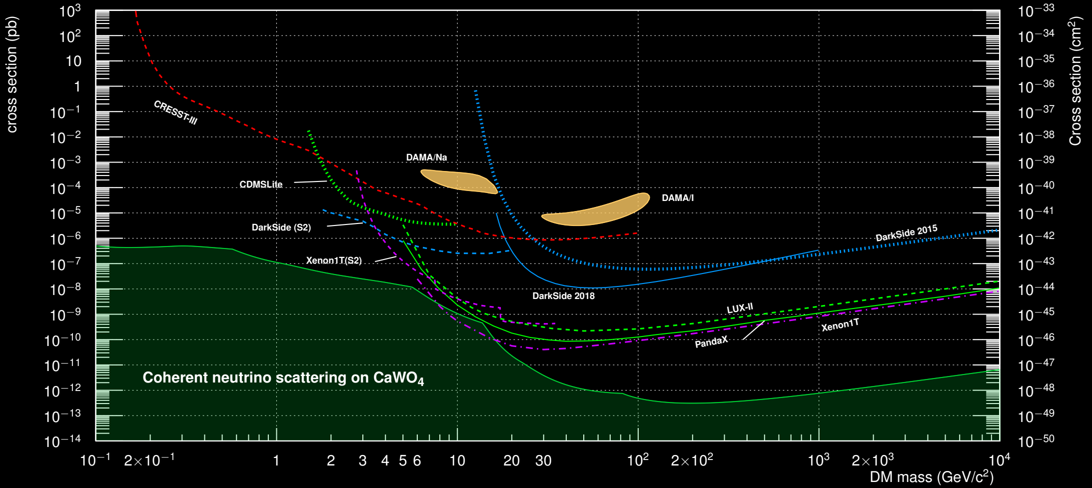

State of the art

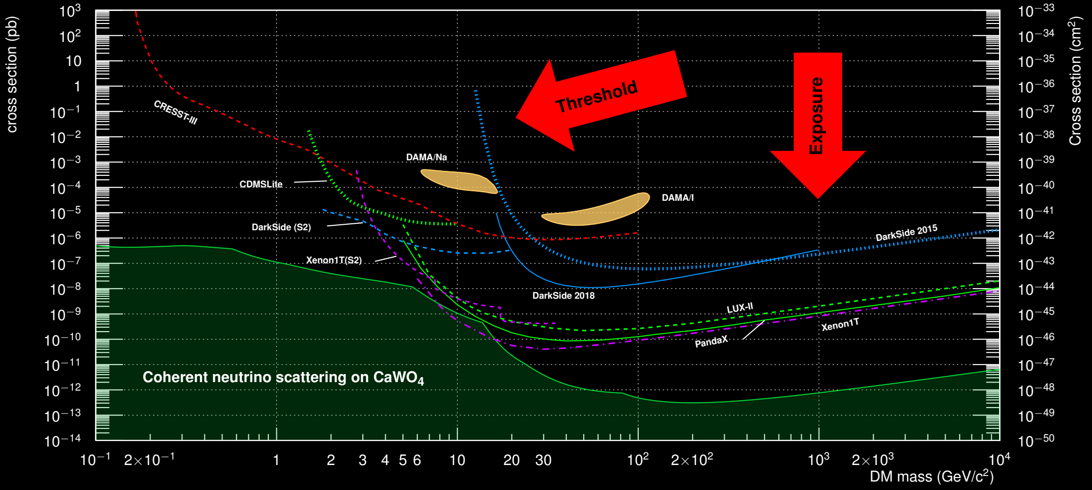

The CRESST experiment

CRESST experiment

Cryogenic Rare Event Search with Superconducting Thermometers

- CRESST is a cryogenic experiment for direct detection of DM.
- Detector target = $CaWO_4$ scintillating crystals
- Simultaneous measurement of the phonon signal in the CaWO4 crystal and the scintillation light provides particle discrimination on an event-by-event basis
- Low energy threshold ($\sim$30 eV)
- Good energy resolution
- Best suited for low dark matter search

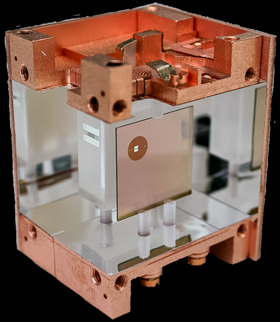

CRESST experiment

CRESST is located at Laboratori Nazionali del Gran Sasso (LNGS, Italy)

Rock overburden $\sim$1400m in all directions (3800 m.w.e.)

Muon flux reduced of a factor 10^{-6}

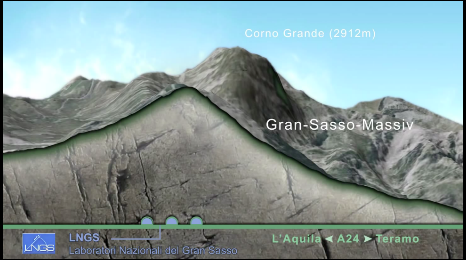

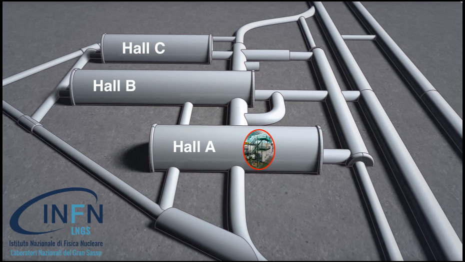

CRESST detector

$CaWO_4$ crystal
Phonon Detector
Energy

Silicon on Sapphire
Light Detector
Radiation

Transition
Edge
Sensor

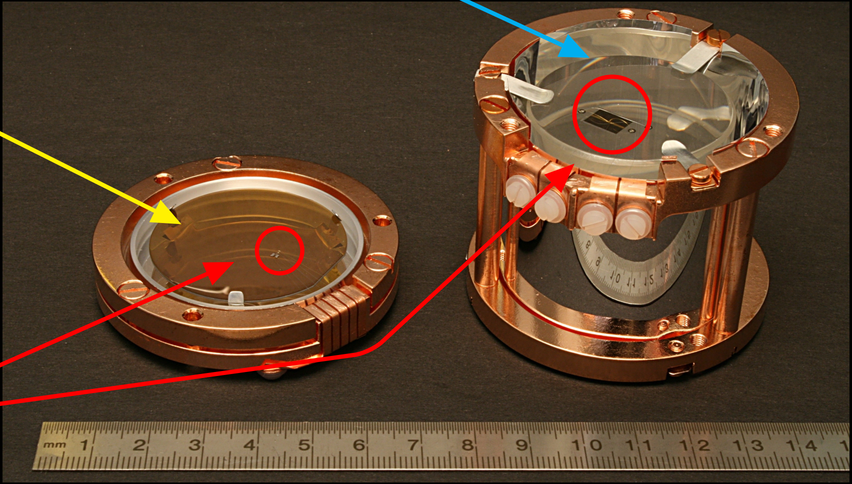

Cryogenic setup

- Dilution refrigerator
- Operating temperature ∼15mK
- Carousel with detector modules

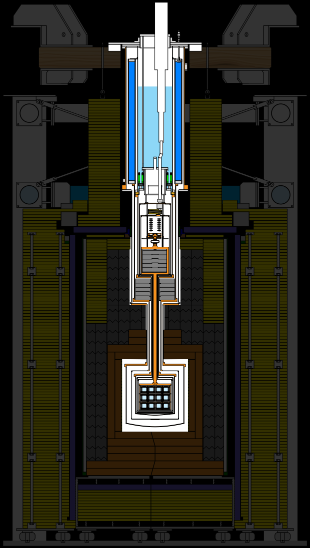

CRESST setup

- Polyethylene shield (2 layer) for neutrons' thermalisation
- Lead shield for beta/gamma radiation
  - extremely difficult to get rid of unstable isotope ^{210}Pb
- Radio pure copper shield for βs and γs from lead shield
- Muon veto
- Radon box

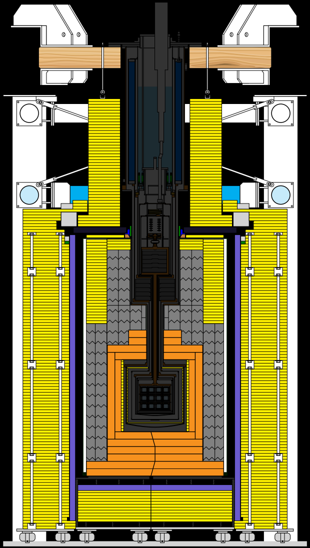

Cryogenic detector

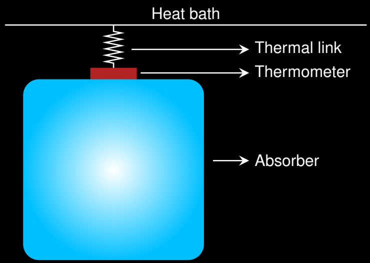

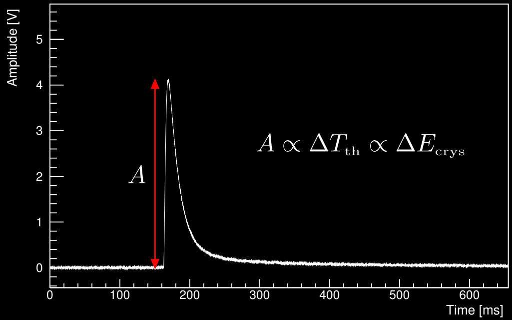

$$\Delta T_{th} = \frac{\Delta E_{th}}{C_{th}} \propto \frac{\varepsilon \Delta E_{crys}}{C_{th}}$$

ε Phonon efficiency collection

C_{th} Thermometer Thermal Capacity

Transition Edge Sensor

Thin layer of Tungsten working in its transition between the normal and the superconducting phase.

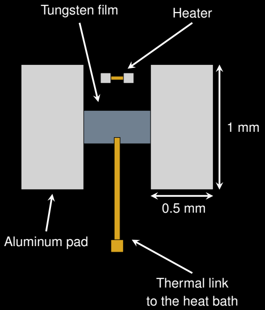

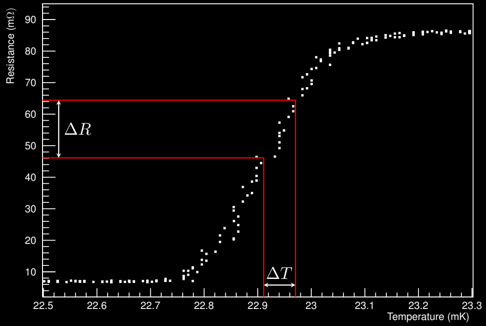

- Aluminum pads to maximize the phonon collection
- Heater for TES energy calibration

$$E \sim \text{keV} \Rightarrow \Delta T \sim \mu\text{K} \Rightarrow \Delta R \sim \text{m}\Omega$$

TES read-out circuit

Because of its small resistance TES has to be operated with very tiny currents.

For this reason, the TES readout is done with a SQUID (Superconducting QUantum Interference Device)

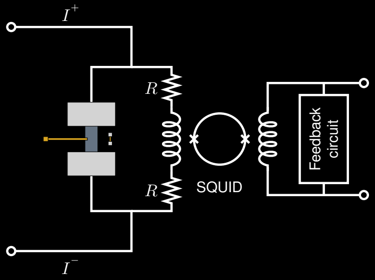

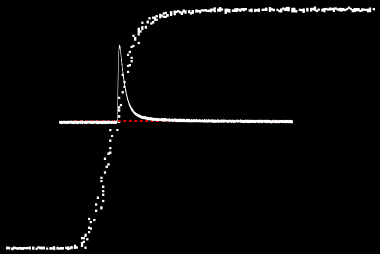

TES read-out circuit

Because of its small resistance TES has to be operated with very tiny currents.

For this reason, the TES readout is done with a SQUID (Superconducting QUantum Interference Device)

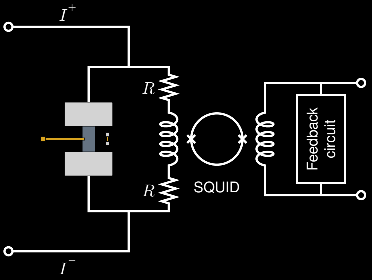

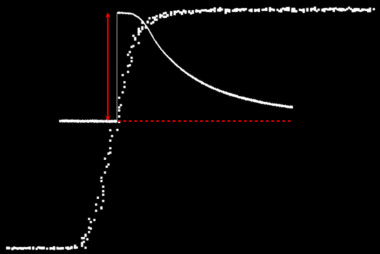

Limitation

The TES dynamic range is very small and it can result in saturated pulses and loss of information.

TES read-out circuit

Because of its small resistance TES has to be operated with very tiny currents.

For this reason, the TES readout is done with a SQUID (Superconducting QUantum Interference Device)

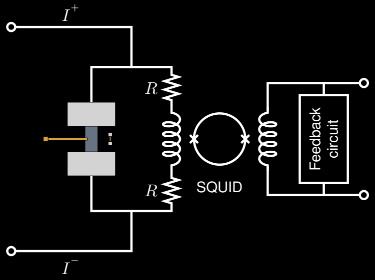

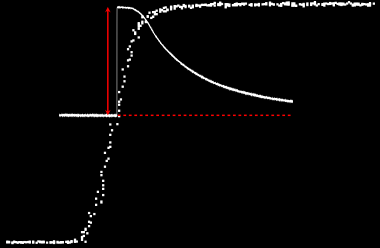

Limitation

The TES dynamic range is very small and it can result in saturated pulses and loss of information.

Truncated Fit Solution

This problem is overcome with the Truncated Fit procedure. The Fit is done with only points from the linear region.

Working principle

Phonon detector

Precise energy measurement ~90% total energy

- Almost particle independent

Light Detector

Few % total energy

- Particle dependent
- Particle discrimination

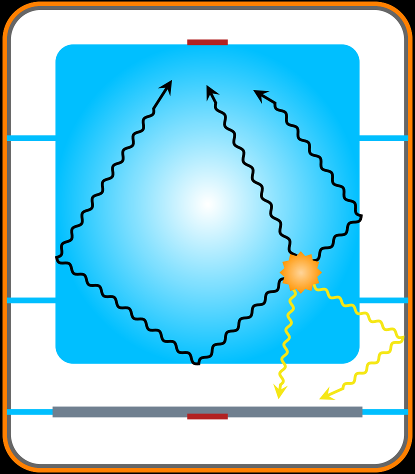

Event discrimination

Particle discrimination done defining the variable

$$\boxed{\mathrm{LY} = \frac{\text{Energy in the Light channel}}{\text{Energy in the Phonon channel}}}$$

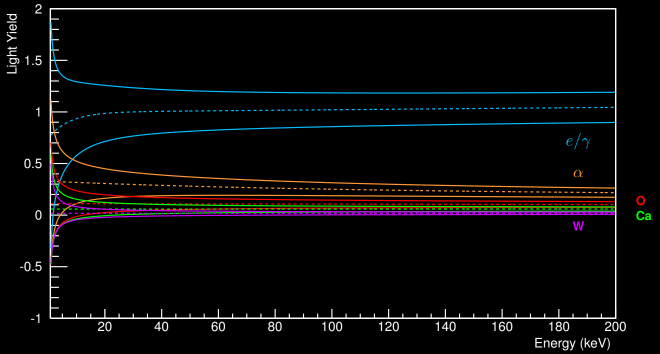

$$\mathrm{QF}^x(E) = \frac{\text{Light produced by } x \text{ when depositing } E}{\text{Light produced by } e/\gamma \text{ when depositing } E}$$

CRESST results

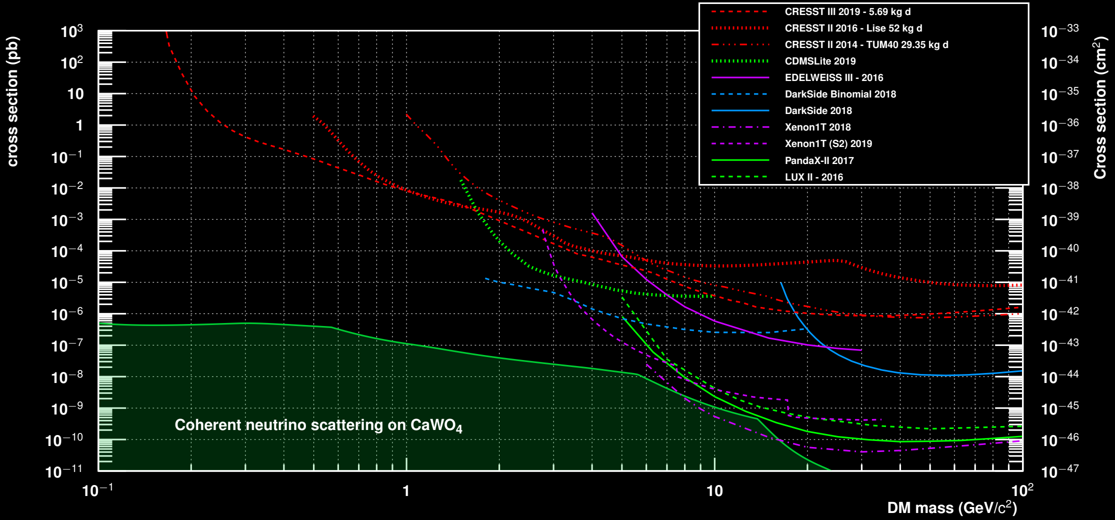

The Yellin method for Exclusion limit computation

The CRESST exclusion analysis is traditionally based on the Yellin method.
This method uses only the signal shape and no knowledge of the background is needed to extract a limit.

- all the events are assumed as signal events
- we search for the interval x_i with the largest area

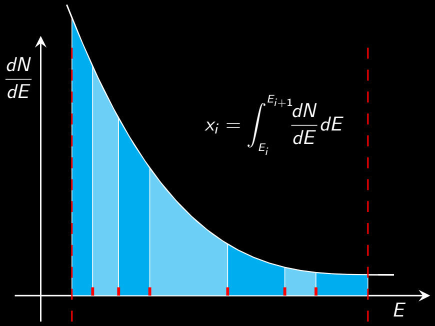

The Yellin method for Exclusion limit computation

The CRESST exclusion analysis is traditionally based on the Yellin method.
This method uses only the signal shape and no knowledge of the background is needed to extract a limit.

- all the events are assumed as signal events
- we search for the interval x_i with the largest area
- we define $C_0(x, \sigma)$ as the probability that a random experiment gives a Maximum Gap smaller than x_{max} in a fraction C_0 of experiments.
- the cross section is changed until a confidence level C_0 is achieved

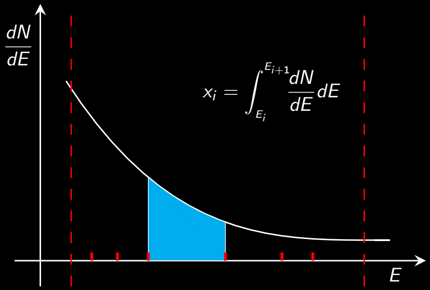

The Yellin method works in 1D and is a conservative approach to extract a limit.

Goal of this work

In this work I propose a different approach to the CRESST exclusion analysis, based on the Extended Maximum Likelihood instead of the Yellin method.

The use of the Extended Likelihood has some advantages:

- Discovery and Exclusion method
- Naturally suited for multi dimensional analysis
- Multiple detectors combination

Combining detectors allows to obtain limits with larger exposure improving the sensitivity for Dark Matter.

Run33 Detector design

CRESST Run33 (2013-2015) is the Run with the largest exposure for single module ($\sim$ 160 kg day)

Standard Design
- VK31
- VK32
- VK33
- VK34
- Verena
- Daisy

Small Carrier Design
- Anja
- Zora
- Frederika
- Lise
- Wibke

Beaker Design
- VK27
- VK28

Carrier Design
- TUM29
- TUM38

Stick Design
- TUM40

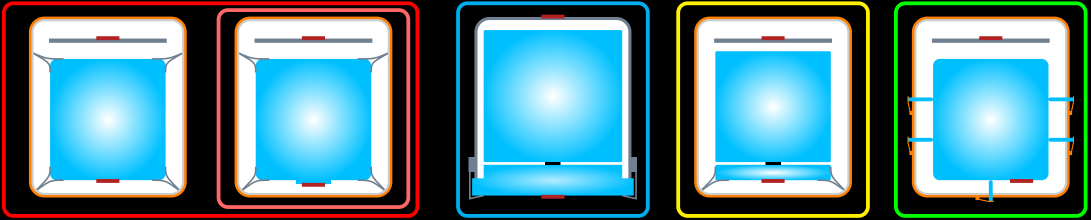

- Different detector design
- Different radio purity
- Different working point and response

$\Rightarrow$ Dedicated study for each module to found the ones with the suitable performances.

Additional Likelihood by-product

https://dx.doi.org/10.1140/epjc/s10052-012-1971-8

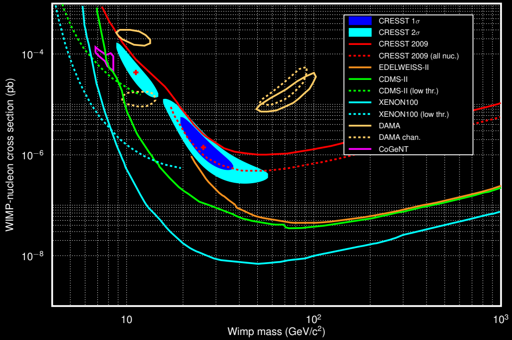

In 2012, the CRESST Run 32 results showed a 4σ excess of events in the acceptance region that could not be explained in terms of known backgrounds.

The Dark Matter interpretation of this excess produced two 90% $C.L.$ contours (*islands*) in the Cross Section - Dark Matter mass plane.

The use of fully active modules in successive runs removed the excess events and partially excluded these regions.

With the Likelihood approach the best test of the *island* in the CRESST framework can be obtained.

CRESST Data Analysis

Datasets

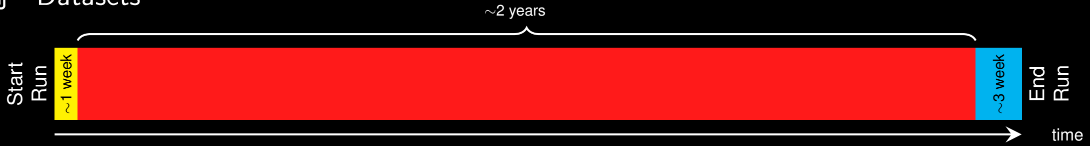

Gamma calibration

Energy calibration with the 122 keV gamma-line from ^{57}Co source

Data

Physics run used for the DM analysis (data quality cuts & high level analysis)

Neutron calibration

Study of the response of every individual detector module to neutron-induced nuclear recoils for a precise determination of QFs as they can vary between different crystals O(10%)

Datasets

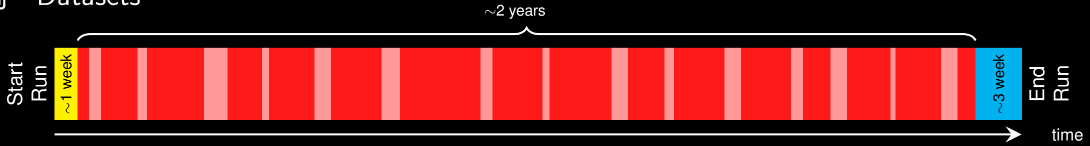

Gamma calibration

Energy calibration with the 122 keV gamma-line from ^{57}Co source

Data

Physics run used for the DM analysis (data quality cuts & high level analysis)

Neutron calibration

Study of the response of every individual detector module to neutron-induced nuclear recoils for a precise determination of QFs as they can vary between different crystals O(10%)

Training set

The 20% of the physics data is randomly selected and used to define the cuts. After the cuts are optimized on the training data are they exported unchanged to the full dataset

Pulse types

Control Pulses

Large heater pulses needed to monitor the TES working point

Test Pulses

Heater pulses with small and varying amplitudes to export the calibration in the whole data set

Empty Baselines

Acquired with artificial trigger and needed for a precise measurement of the noise and efficiency calculation

Particle pulses

Real trigger events due to particle interactions in the detector

Control Pulses

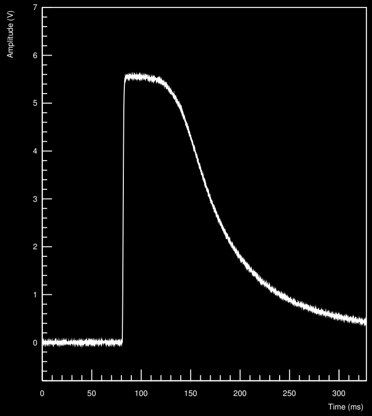

Pulse types

Control Pulses

Large heater pulses needed to monitor the TES working point

Test Pulses

Heater pulses with small and varying amplitudes to export the calibration in the whole data set

Empty Baselines

Acquired with artificial trigger and needed for a precise measurement of the noise and efficiency calculation

Particle pulses

Real trigger events due to particle interactions in the detector

Test Pulses

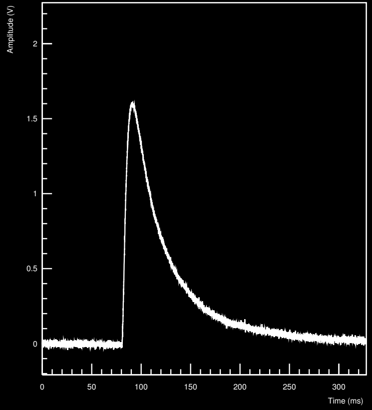

Pulse types

Control Pulses

Large heater pulses needed to monitor the TES working point

Test Pulses

Heater pulses with small and varying amplitudes to export the calibration in the whole data set

Empty Baselines

Acquired with artificial trigger and needed for a precise measurement of the noise and efficiency calculation

Particle pulses

Real trigger events due to particle interactions in the detector

Empty Baselines

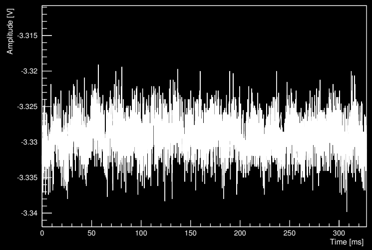

Pulse types

Control Pulses

Large heater pulses needed to monitor the TES working point

Test Pulses

Heater pulses with small and varying amplitudes to export the calibration in the whole data set

Empty Baselines

Acquired with artificial trigger and needed for a precise measurement of the noise and efficiency calculation

Particle pulses

Real trigger events due to particle interactions in the detector

Particle Pulses

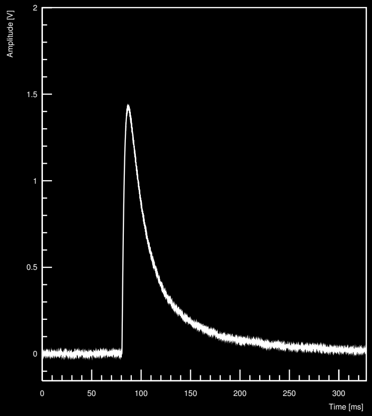

Analysis chain

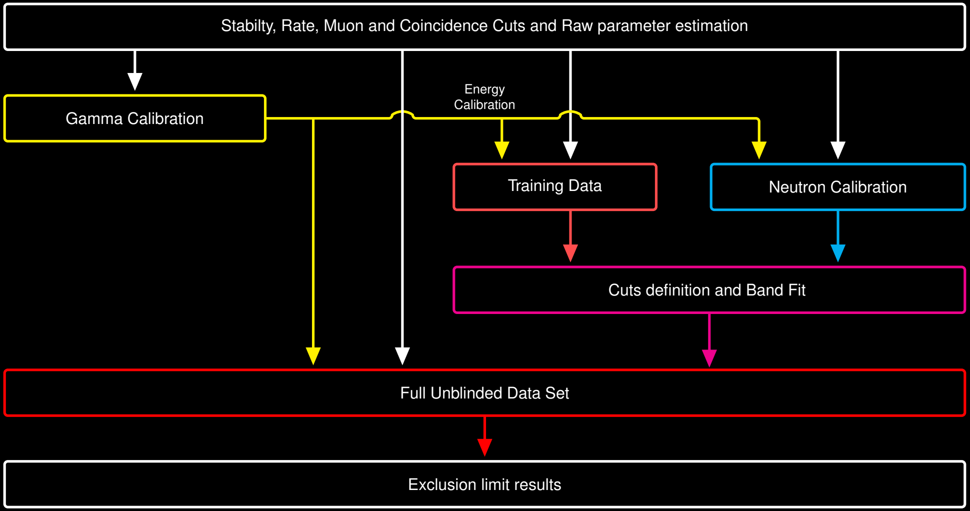

Stability & Rate cuts (VK31)

To remove time periods in which the TES is out of the correct working point.
Done with the control pulse distribution.

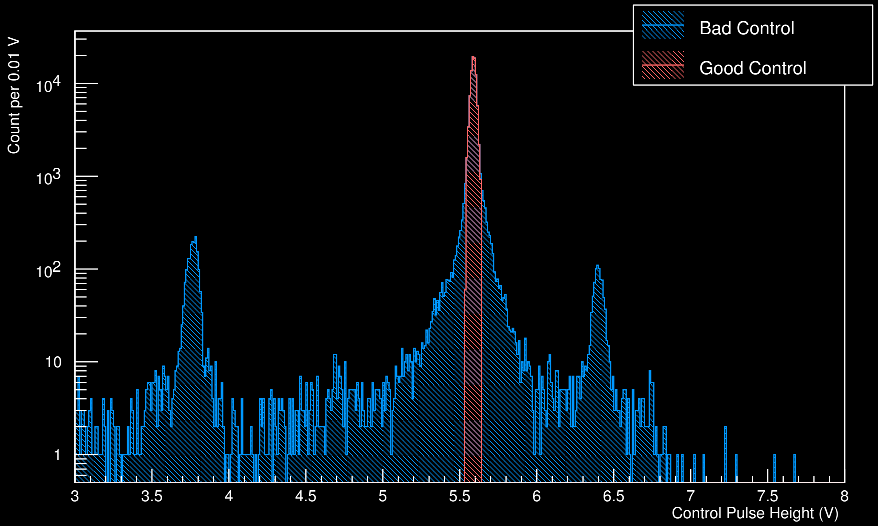

Stability & Rate cuts (VK31)

To remove high trigger rate periods (electronics and environmental disturbances..)

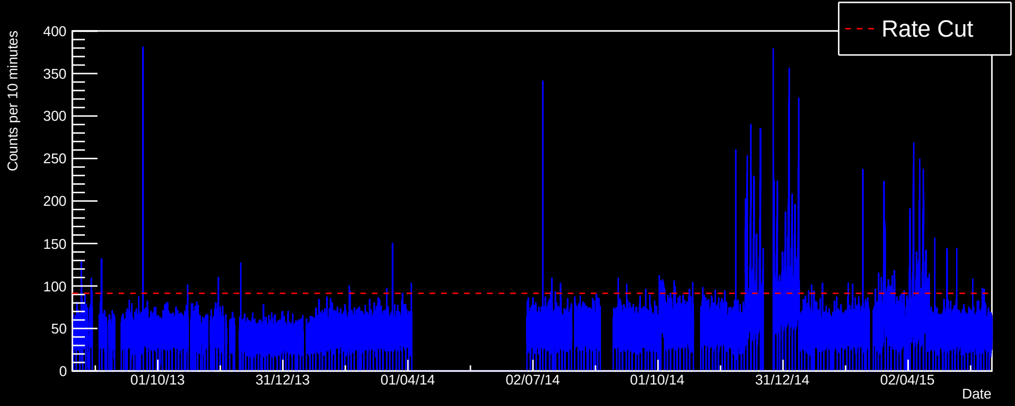

Muon & Detectors Coincidence cuts

These cuts remove events in coincidence with signals in other detectors or in the muon veto panels.

The detector coincidence is particularly relevant to reject multi-detector hits due to neutrons.

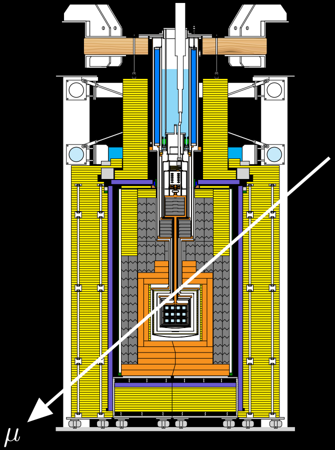

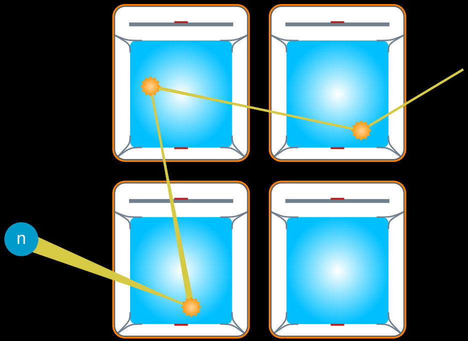

Raw Parameter estimation

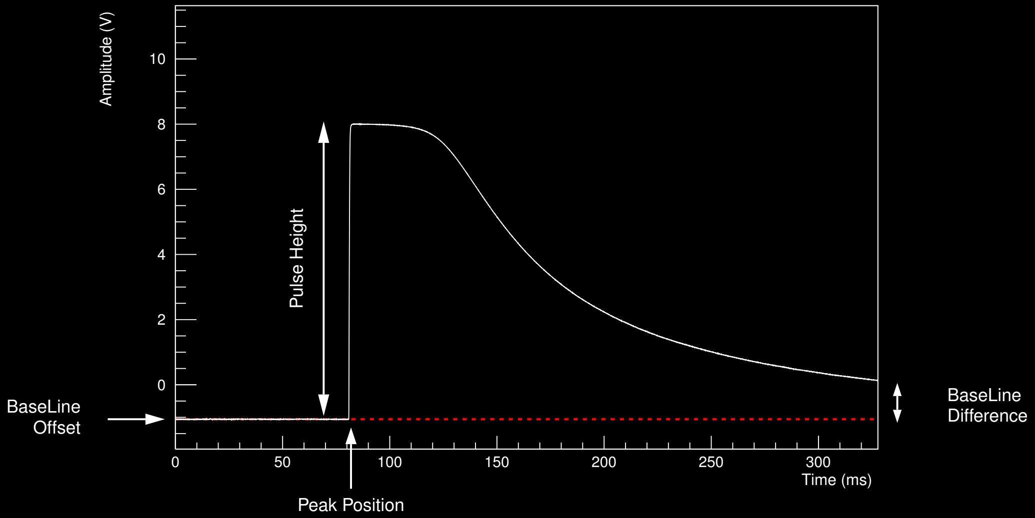

Template creation (VK31)

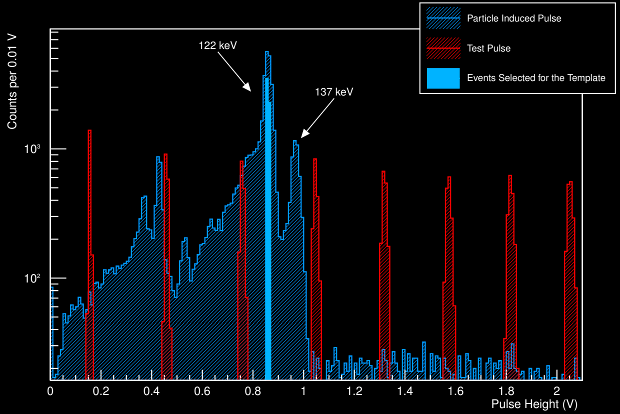

$\frac{1}{n}\sum_i$

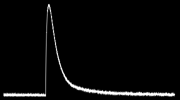

$\|$

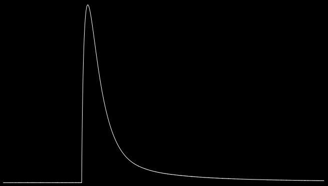

Fit procedure

The template amplitude is scaled and the position is adjusted to match the pulse.

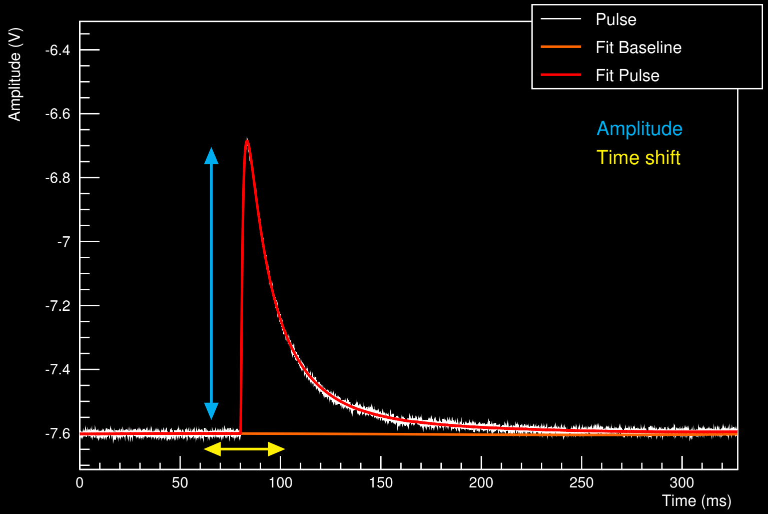

Fit procedure

The template amplitude is scaled and the position is adjusted to match the pulse.

The procedure works until we fit pulses without non-linear or saturation effects.

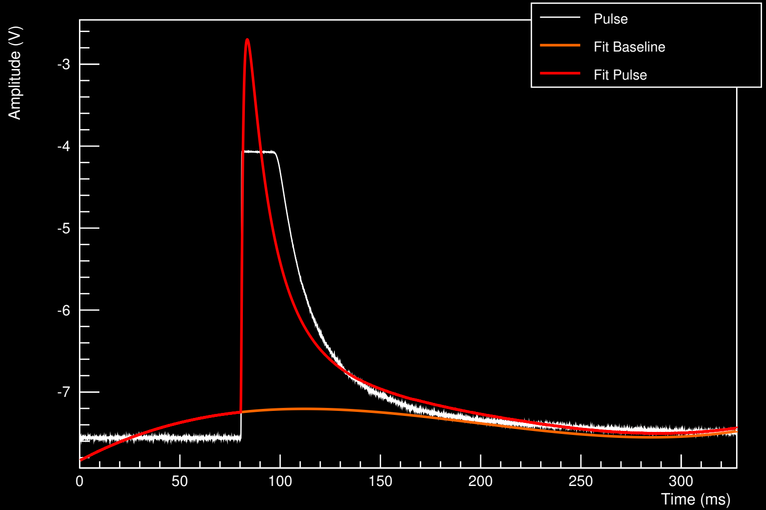

Truncated fit procedure

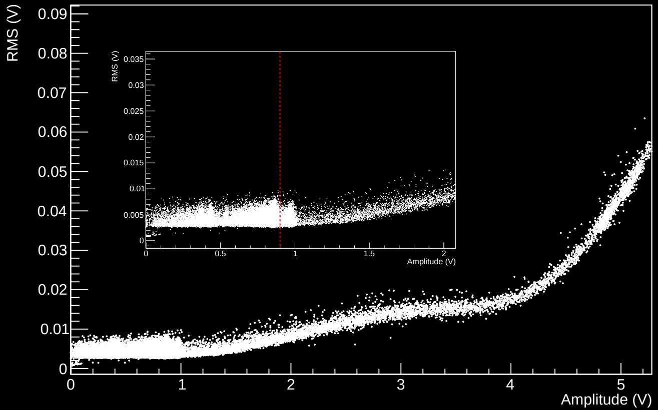

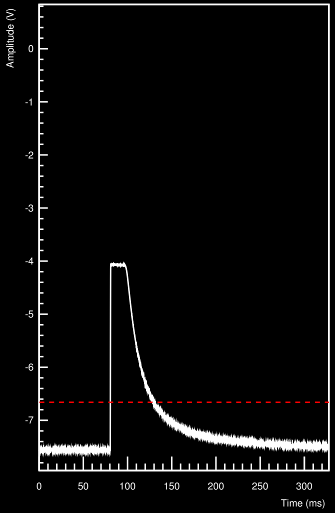

Truncated fit procedure

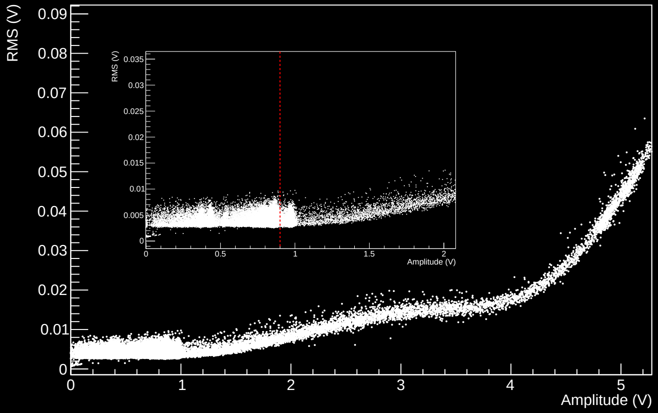

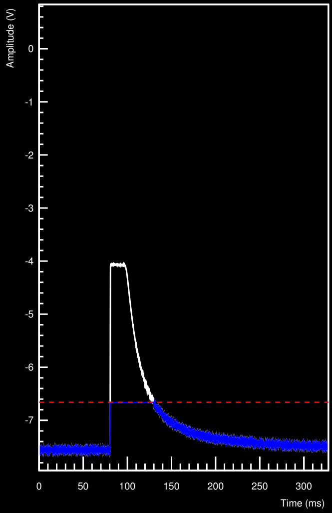

Truncated fit procedure

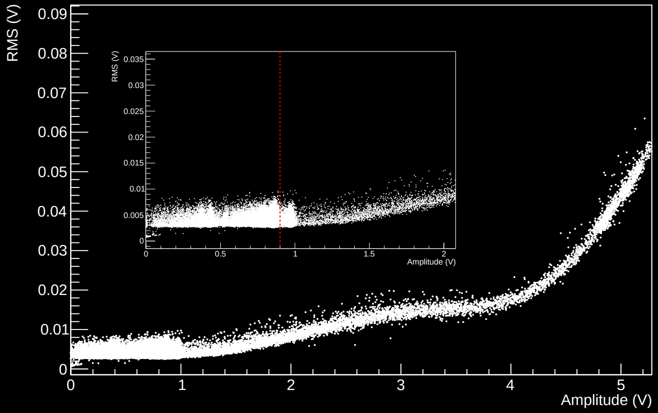

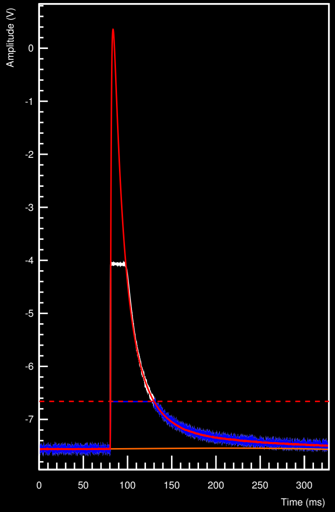

Test Pulse Energy Calibration

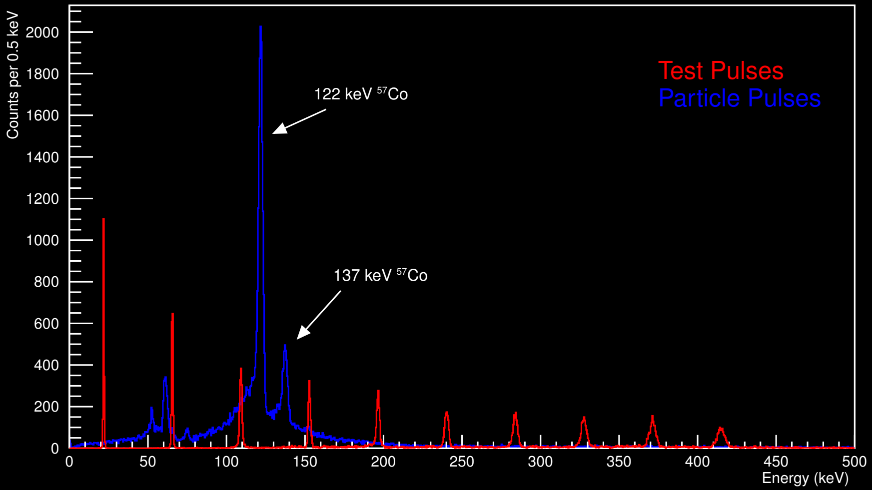

Training Set Analysis

Training set analysis: Light vs Phonon Pulse Heights (Verena)

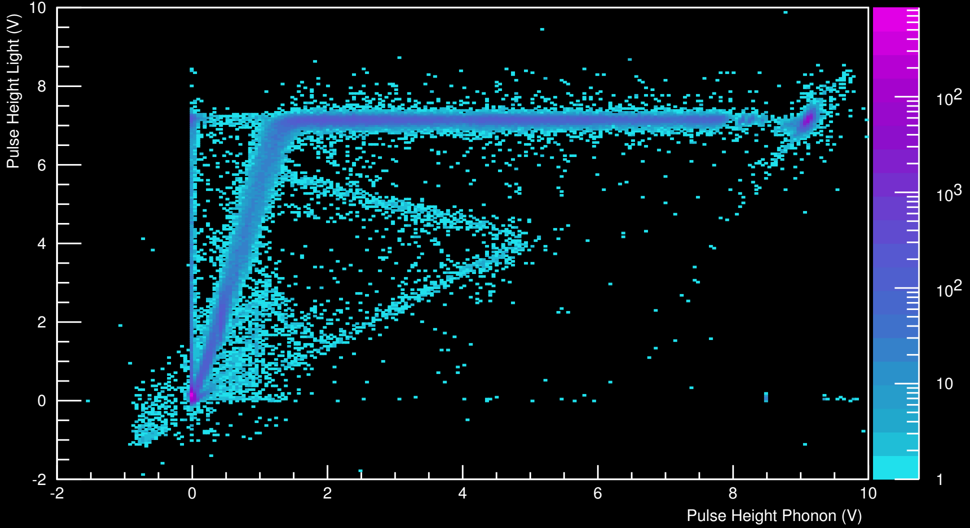

Training set analysis: populations study (Verena)

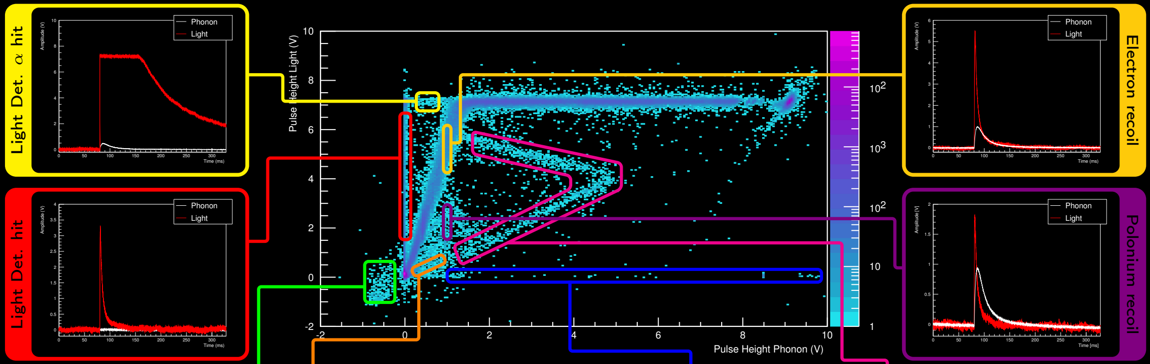

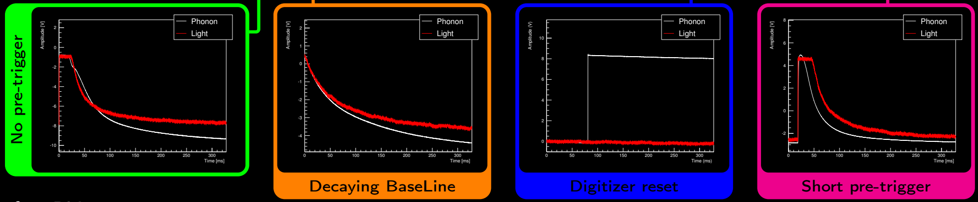

Study of the different population done for each of the 12 detector analysed.

Training set analysis: gamma tilt correction (TUM40)

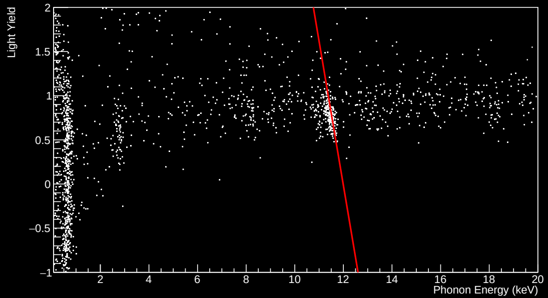

After correction

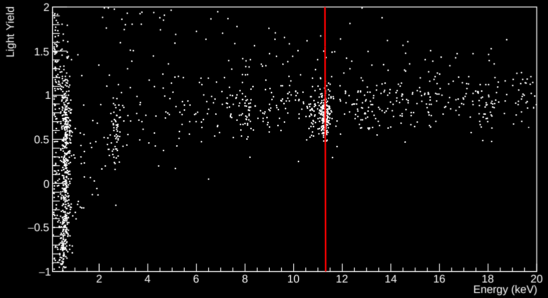

The light and phonon channel anti-correlation causes a tilt of the γ lines which can be corrected.

$$E = [1 - \eta(1 - LY)]\, E_p$$

Training set analysis: gamma tilt correction (TUM40)

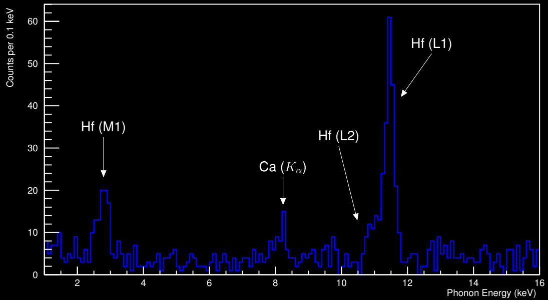

After correction

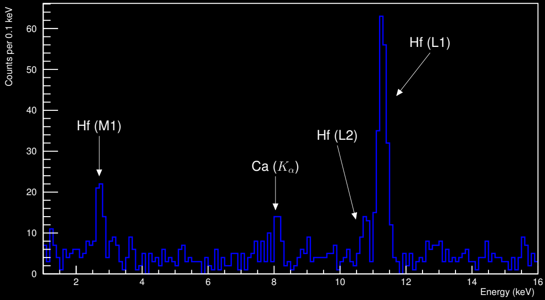

The light and phonon channel anti-correlation causes a tilt of the γ lines which can be corrected.

$$E = [1 - \eta(1 - LY)]\, E_p$$

$$^{182}W(p,\alpha)^{179}Ta$$

$$^{179}Ta + e^- \xrightarrow{1.82y} {}^{179}Hf + \nu_e$$

Training set analysis: Cuts effect (Verena)

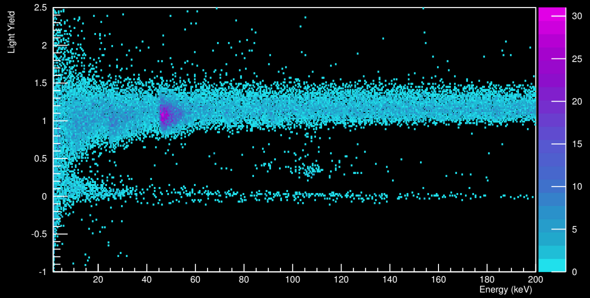

After Cuts and Correction

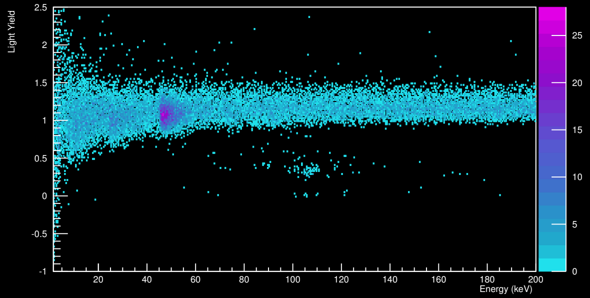

The cuts remove most of the events in the nuclear recoil band.

Since the cuts have been optimized on data with almost no nuclear recoil, they could remove most of the nuclear recoil events.

Check cuts on Neutron data (Verena)

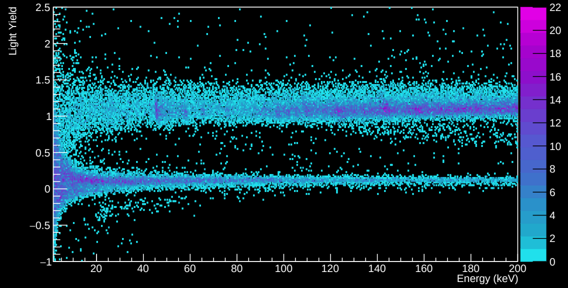

After Cuts and Correction

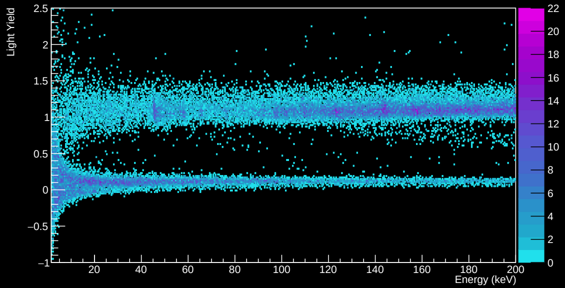

The cuts are optimized on the training dataset and applied without any change to neutron calibration data. The Nuclear recoil bands are full of events.

Cut efficiency estimation

An important step of the analysis is the Cut efficiency estimation as function of the energy.
This is done adding a scaled template to an empty baseline.
The simulation of the different energies is done varying the template amplitude.

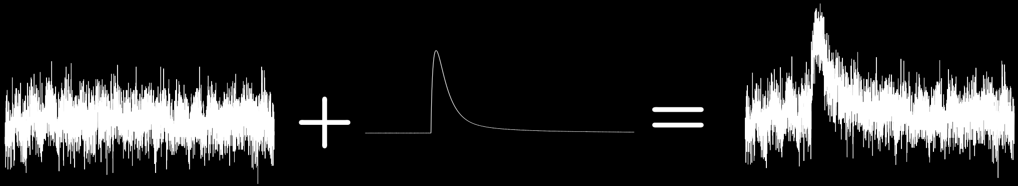

Cut efficiency (Frederika)

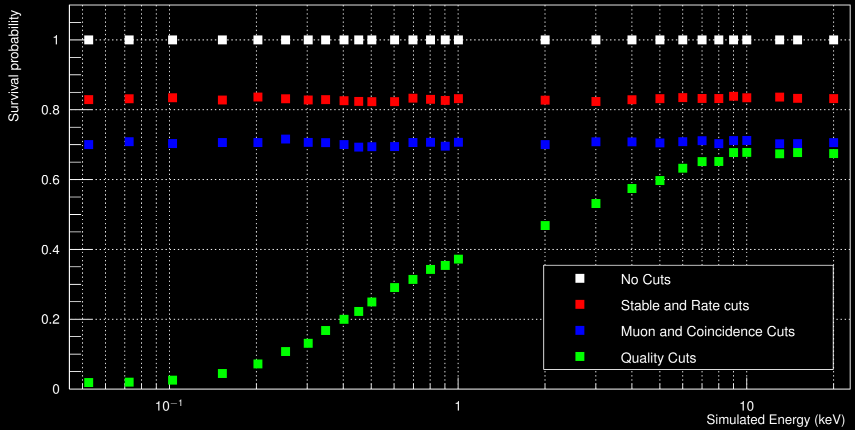

Threshold measurement (Frederika)

The threshold is defined as the value for which 50% of the events are triggered.

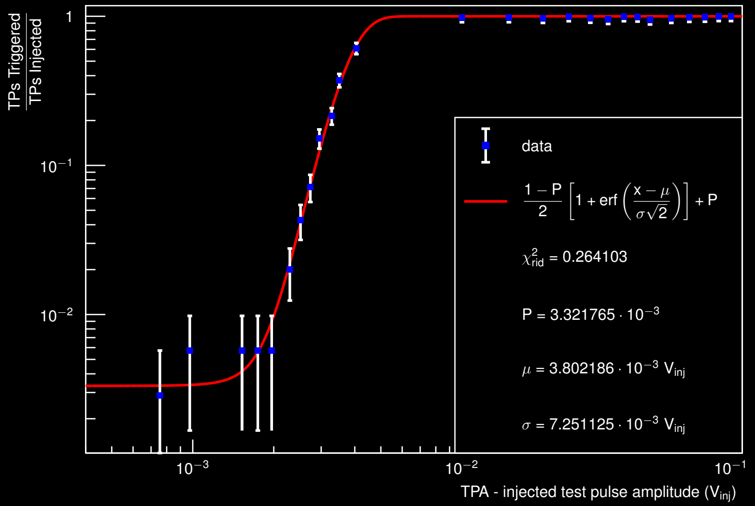

Band Fit

Band fit (Anja)

To better fit the bands, the combined data from the neutron calibration and the training dataset are used.

In this way, more statistics is available, especially in the nuclear recoil bands, which are the one interesting for the Dark Matter search.

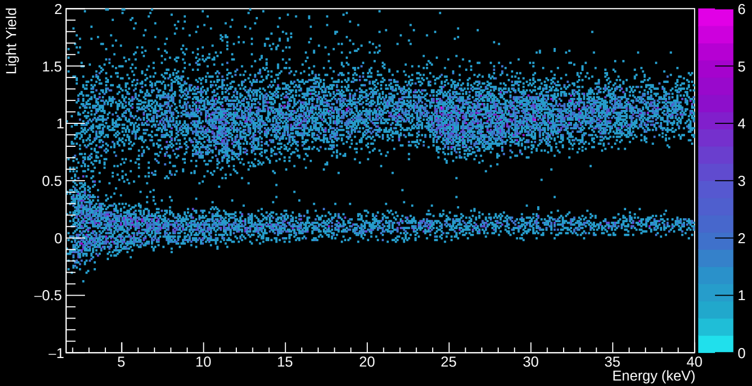

Extended Likelihood description of the band

$$\mathcal{L}^{\text{ext}}_{\text{tot}}(\Theta|x) = e^{-\mathcal{N}} \prod_{i}^{N} \rho(x_i \,|\, \Theta)$$

$$\rho = \rho_e + \rho_\gamma + \rho_{nr} + \rho_\chi$$

θ accounts
for more than 30 parameters

$$\Theta = (\sigma_\chi, m_\chi, \theta)$$

$$\mathcal{N} = \int_A \rho(x_i \,|\, \Theta) dA$$

Extended Likelihood description of the band

$$\mathcal{L}^{\text{ext}}_{\text{tot}}(\Theta|x) = e^{-\mathcal{N}} \prod_{i}^{N} \rho(x_i \,|\, \Theta)$$

$$\rho = \rho_e + \rho_\gamma + \rho_{nr} + \cancel{\rho_\chi}$$

Band fit without the Dark Matter density function

$$\Theta = (\cancel{\sigma_\chi}, m_\chi, \theta)$$

θ accounts for more than 30 parameters

$$\mathcal{N} = \int_A \rho(x_i \,|\, \Theta) dA$$

Band fit (Anja)

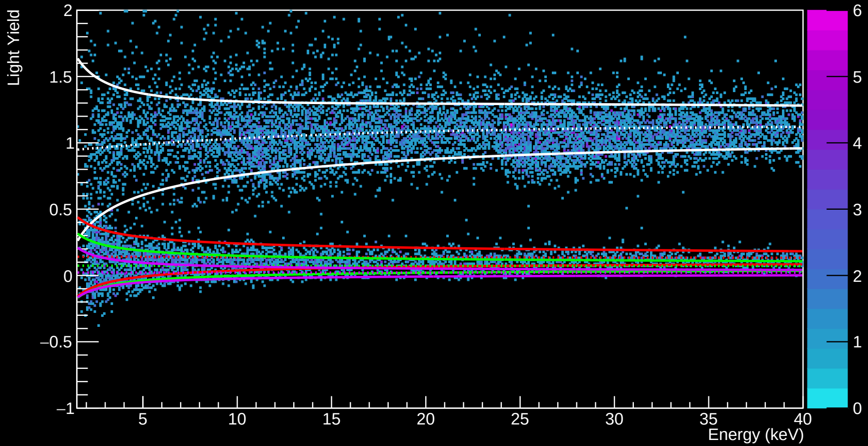

Extended Likelihood Exclusion limits and Physics results

Exclusion limit results

- In total 12 detector modules have been analysed
- Exposure for a single module ∼160 kg day
- A subset of 5 modules has been selected for the analysis based on background, resolution, noise, and live-time

Detector	$\sigma_{P,0}$ (keV)	$\sigma_{L,0}$ (keV)	Threshold (keV)	Live Exposure (kg days)
TUM40	0.0793	0.241	0.8	129.22
Frederika	0.109	0.236	0.759	137.01
Anja	0.126	0.190	1.24	159.13
Verena	0.103	0.281	1.54	164.83
Lise	0.0598	3.23	1 .0	158.67

Extended Likelihood Exclusion limit

$$\mathcal{L}^{\text{ext}}_{\text{tot}}(\Theta|x) = e^{-\mathcal{N}} \prod_{i}^{N} \rho(x_i \,|\, \Theta)$$

$$\Theta = (\sigma_\chi, m_\chi, \theta)$$

$$\Uparrow$$

Dark Matter reintroduced
for the exclusion limit calculation

$$\lambda(\chi) = \frac{\mathcal{L}(\sigma_\chi, \hat{\hat{\theta}} \,|\, x_i, m_\chi)}{\mathcal{L}(\hat{\sigma}_\chi, \hat{\theta} \,|\, x_i, m_\chi)}$$

$$q_\sigma = \begin{cases} -2\ln\lambda(\chi) & \sigma_\chi \geq \hat{\sigma}_\chi \\ 0 & \sigma_\chi < \hat{\sigma}_\chi \end{cases}$$

$$p_s = \int_{q_0}^{\infty} f(q_\sigma \,|\, H_\sigma) dq_\sigma$$

$$q_\sigma \sim \chi_1^2 \Rightarrow \sqrt{q_\sigma} \equiv Z \sim \mathcal{N}(0,1)$$

$$\underbrace{\ln\left[\mathcal{L}\left(\sigma_\chi, \hat{\hat{\theta}}|m_\chi, \theta\right)\right]}_{\text{Profiled Likelihood}} = \underbrace{\ln\left[\mathcal{L}\left(\hat{\sigma}_\chi, \hat{\theta}|m_\chi, \theta\right)\right]}_{\text{Best Fit}} + \frac{Z^2}{2}$$

Z is the significance
i.e $Z = 1.282$ for 90% significance

Exclusion limit results

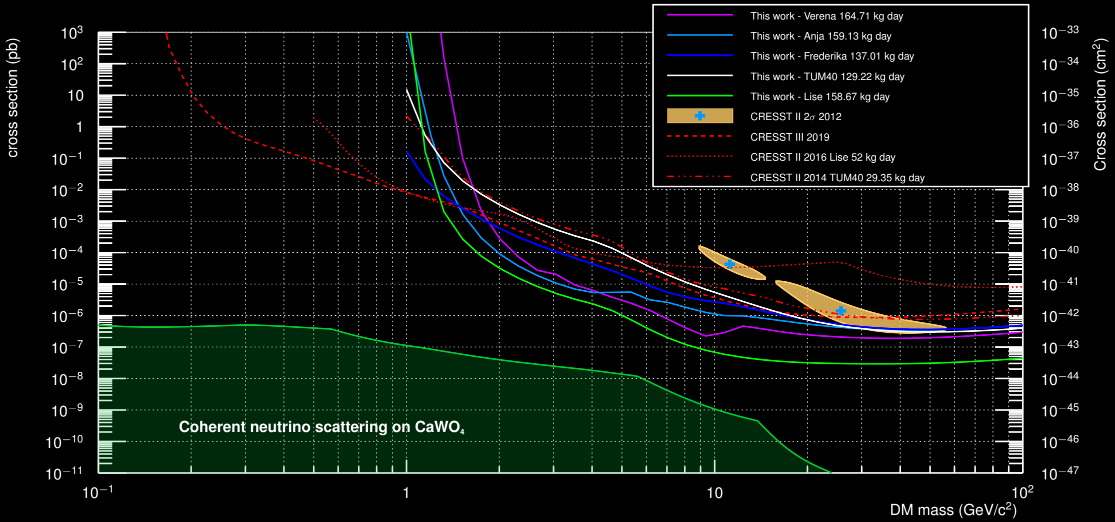

Band Systematic Effects on the Limit

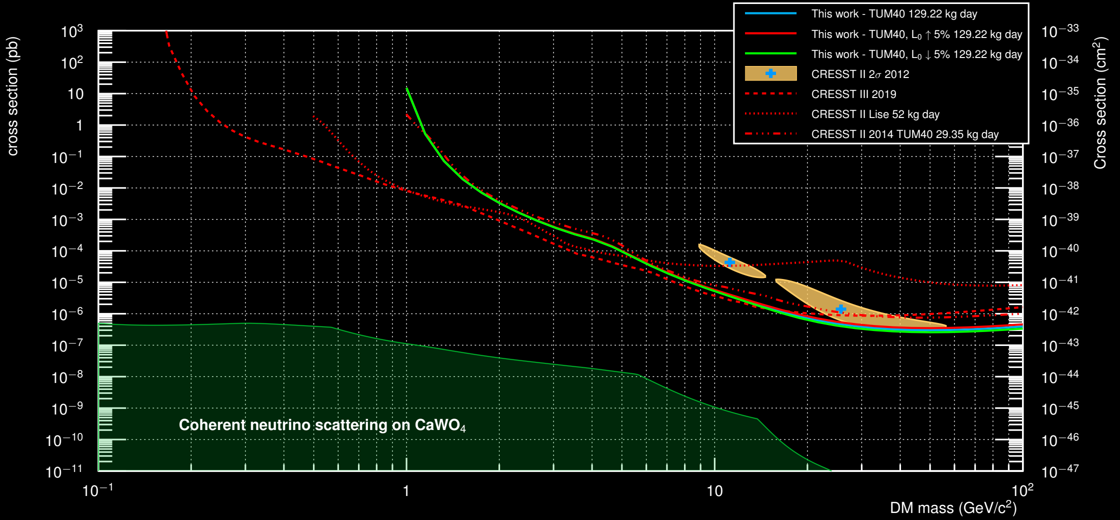

Band Systematic Effects on the Limit

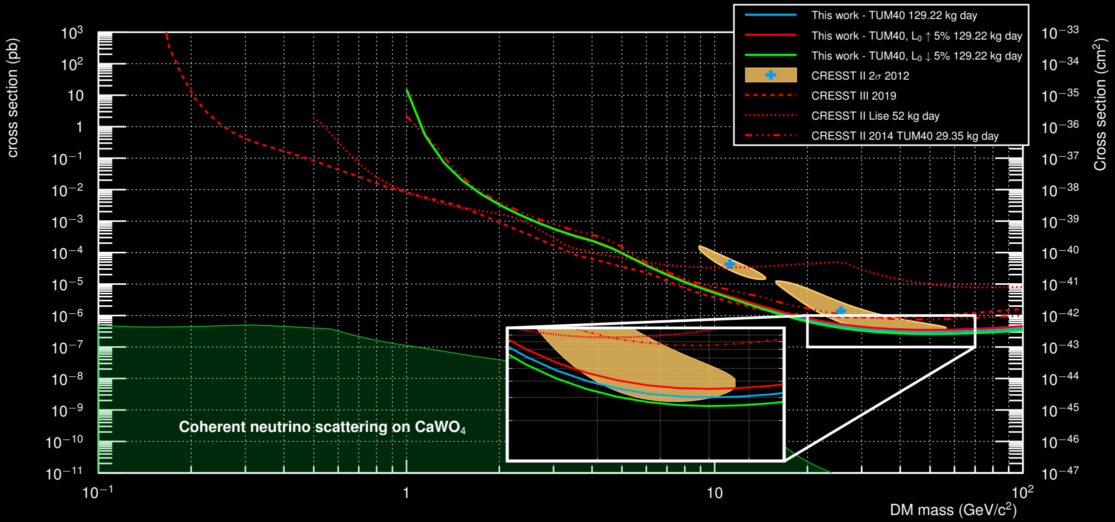

Extended global Likelihood

$$\mathcal{L}_{\text{tot}}^{\text{ext}}(\Theta|x) = e^{-\mathcal{N}_{tot}} \prod_{d}^{D} \left[\prod_{i}^{N_D} \rho_d(x_i \,|\, \Theta) \right]$$

$$\mathcal{N}_{tot} = \sum_{d} \int_{A} \rho_d(x_i \,|\, \Theta) dA$$

Exclusion limit results

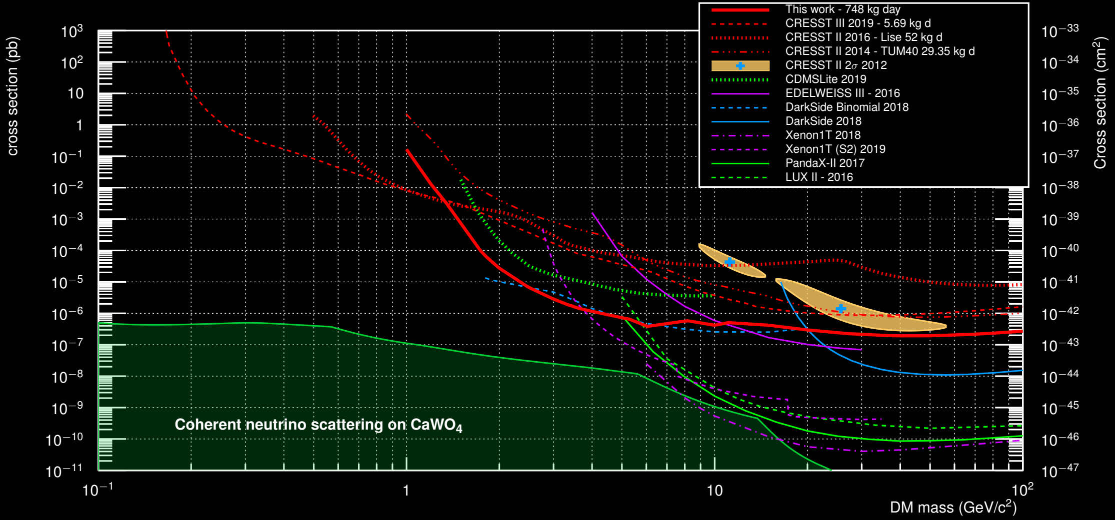

Exclusion limit results

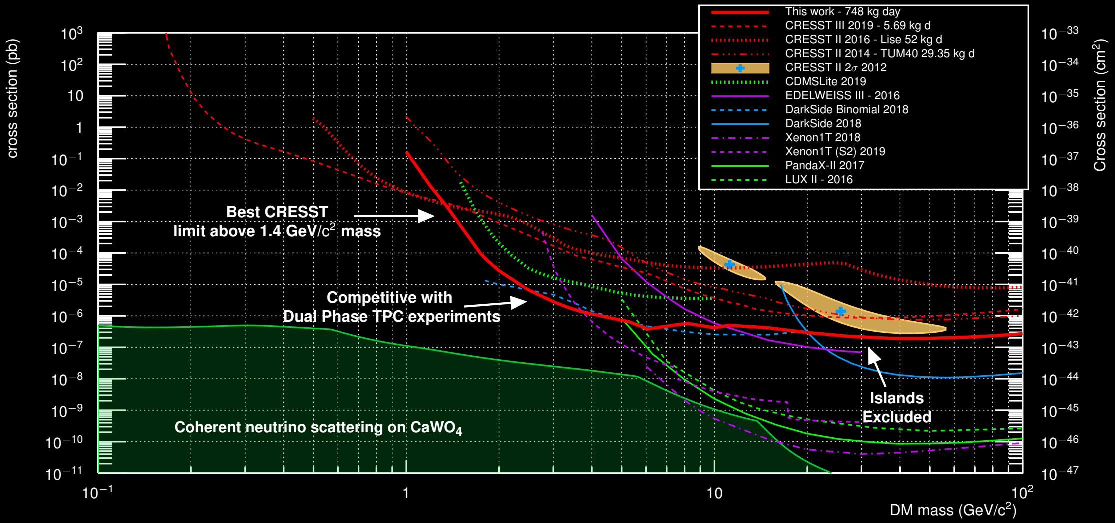

Conclusion

- Thanks to the Likelihood approach, I combined the data from 5 detectors for a total exposure of 748.86 kg days.
- I obtained the CRESST limit with the largest exposure.
- I completely excluded the islands from the 2012 CRESST Run with a Confidence Level of 90%.
- I obtained the best CRESST limit for Dark Matter mass above 1.4 GeV/c^2.
  - Previous CRESST results improved by at least one order of magnitude above 1.5 GeV/c^2.
  - The limit obtained is competitive in the region 1.4 - 4 GeV/c^2.

Outlook

- Increase of the exposure, including more detectors in the analysis;
- Improve the limit calculation including:
  - the systematics uncertainties;
  - MC background simulations;
- Paper with this analysis is in preparation.

Thanks for the attention

Back up Slides

Superconducting QUantum Interference Device

Very sensitive magnetometer used to measure extremely tiny magnetic fields, based on superconducting loops containing Josephson junctions.

Superconducting rings can enclose magnetic flux only in multiples of a universal constant called the flux quantum.

$$\Phi_0 = \frac{h}{2e} = 2.07 \times 10^{15}\ \mathrm{Wb}$$

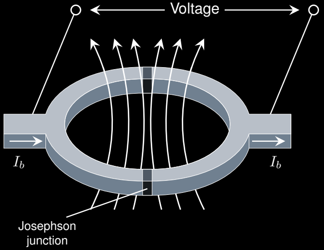

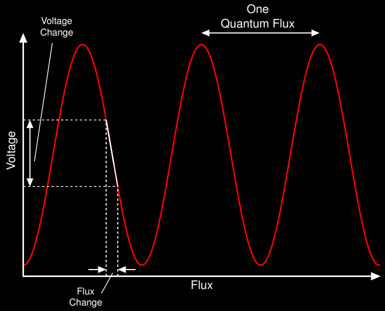

Alpha analysis

The truncated fit procedure is reliable up to 5 MeV and used for the α analysis.

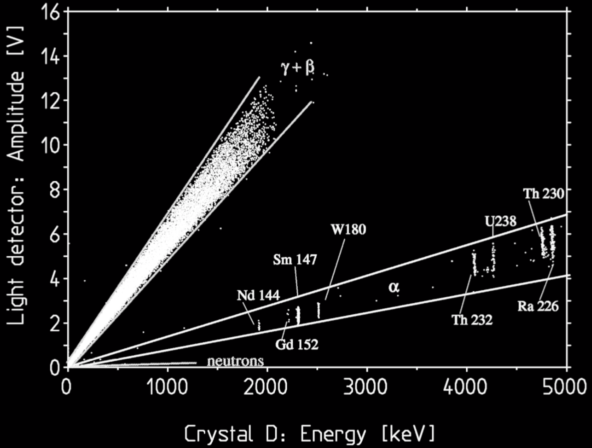

https://journals.aps.org/prc/abstract/10.1103/PhysRevC.70.064606

Time variation effects adjustament

The Test Pulses are used to correct for small temperature variations over time.

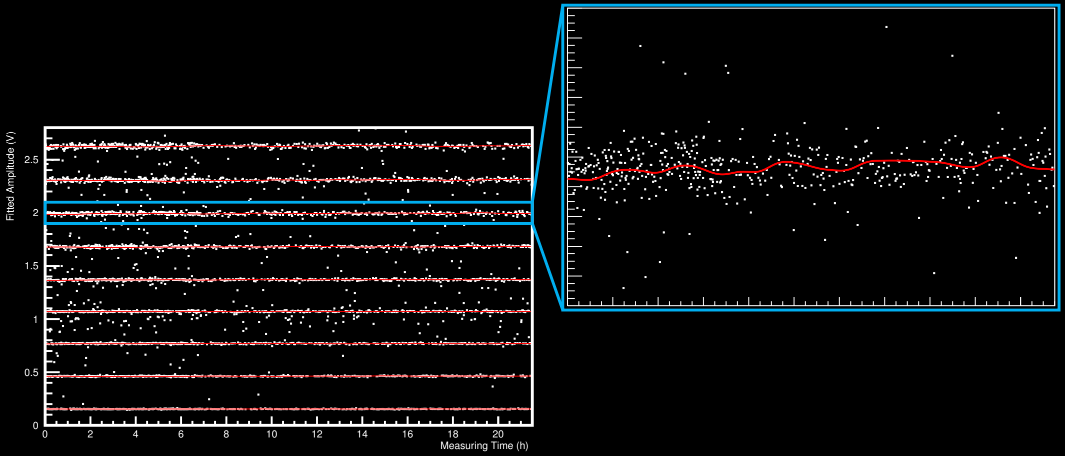

Energy Calibration and CPE

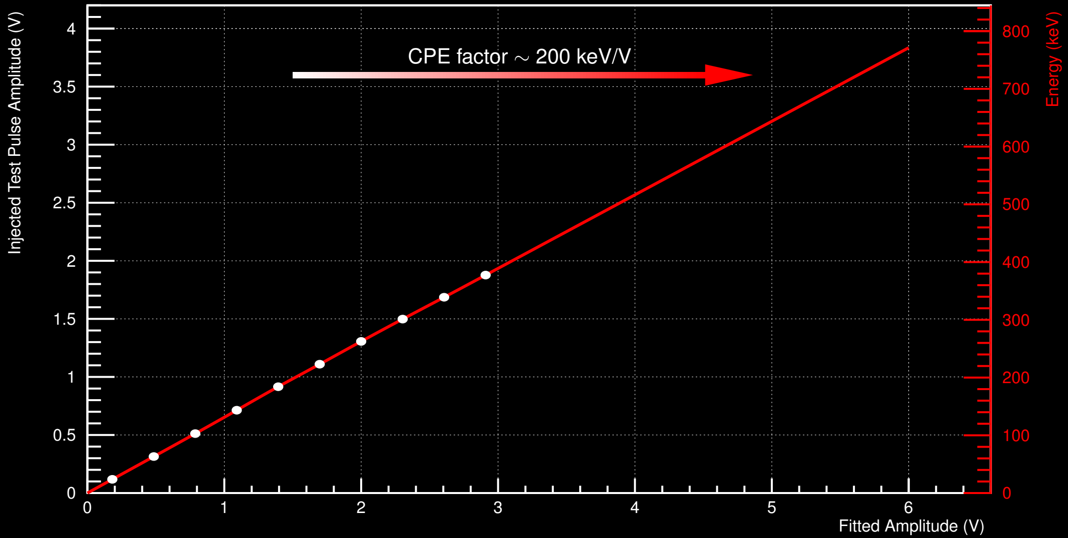

Band Description : Light Mean

$$L_e(E) = \left(L_0 E + L_1 E^2\right)\left[1 - L_2 \exp\left(-\frac{E}{L_3}\right)\right]$$

$$L_\gamma(E) = L_e(E') \text{ with } E' = E\,Q_{\gamma,1} + E^2\,Q_{\gamma,2}$$

$$L_x(E) = \left(L_0 E + L_1 E^2\right) \epsilon\, QF_x \left[1 + f_x \exp\left(-\frac{E}{\lambda_x}\right)\right]$$

First approximation
Non proportionality effect
Crystal specific

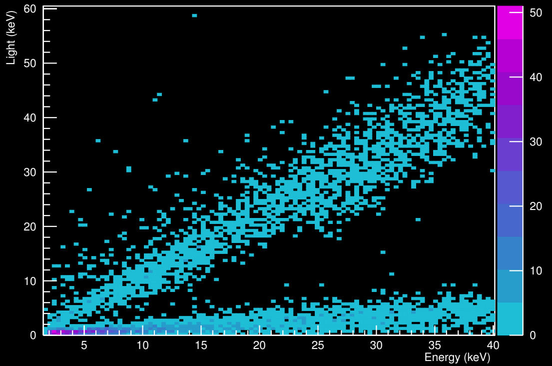

Nucleus	QF_x	f_x	λ_x
O	0.07908 ± 0.00002	0.7088 ± 0.0008	567.1 ± 0.9
Ca	0.05949 ± 0.0078	0.1887 ± 0.0022	802 ± 19
W	0.0196 ± 0.0022	0	∞

https://link.springer.com/article/10.1140/epjc/s10052-014-2957-5

Band Description : Light Width

$$\sigma_P(E) = \sqrt{\sigma_{P,0}^2 + \sigma_{P,1} E}$$

$$\sigma_L(L) = \sqrt{\sigma_{L,0}^2 + S_1 L + S_2 L^2}$$

Parametrization of the energy resolution of phonon and light detectors

$$\sigma_x(L) = \sqrt{\sigma_L + \frac{dL_x}{dE}(E)\sigma_P}$$

Light band width of the x-th species

Band Description : Energy Spectrum

Electron spectrum

$$\frac{dN_e}{dE} = P_0 + P_1 E$$

Neutron spectrum

$$\frac{dN_{n,x}}{dE} = A_{n,x} \exp\left(-\frac{E}{\lambda_x}\right)$$

Beta spectrum

$$\frac{dN_{\beta,i}}{dE} = \mathcal{G}(E, \sigma_P(E)) * C_{\beta,i} \mathcal{T}(E, E_0, Q)$$

Gamma spectrum

$$\frac{dN_{\gamma,i}}{dE} = C_{\gamma,i} \mathcal{G}(E, \sigma_P(E))$$

Density function

$$\rho_x = \frac{dN_x}{dE} \mathcal{G}(L(E), \sigma_{L,x}(E)) \quad , \quad \rho = \rho_e + \rho_\gamma + \rho_n + \rho_\chi$$

Polonium recoil

^{210}Po comes from the ^{222}Rn contamination
^{210}Po decays in α (5.3 MeV) and ^{206}Pb (103 keV).

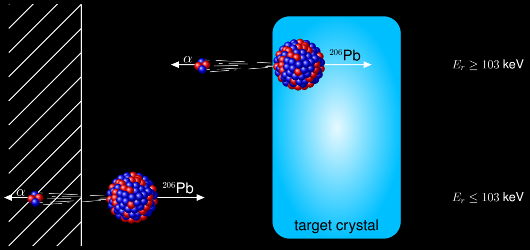

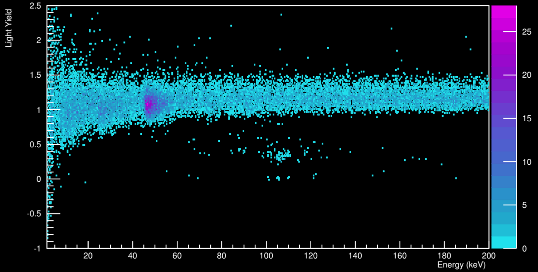

Pulse Height evaluation

The BaseLine is estiamted fitting the first 23% of the recorded pulse whit a linear function. The Pulse Height is obtained as the difference between the pulse maximum and the BaseLine.

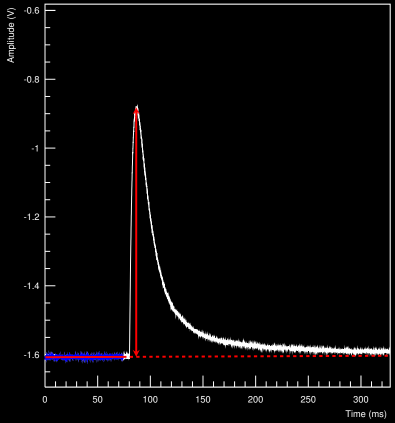

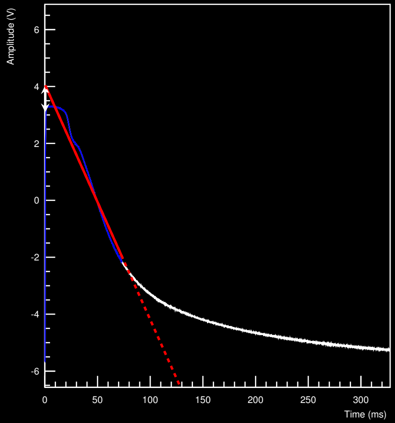

Carrier fit

Pulses from event in the carrier have a shorter decay time. The RMS of the fit is not bad enough to distinguish carrier from particle pulse.

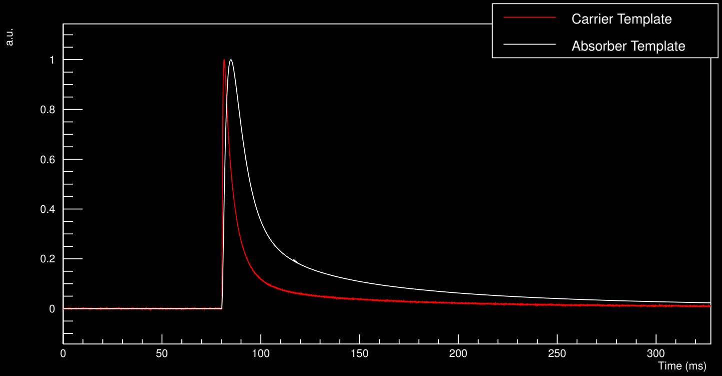

Carrier fit

The variable $\frac{RMS_a - RMS_c}{RMS_a + RMS_c}$ is then defined and used to distinguish between the events.

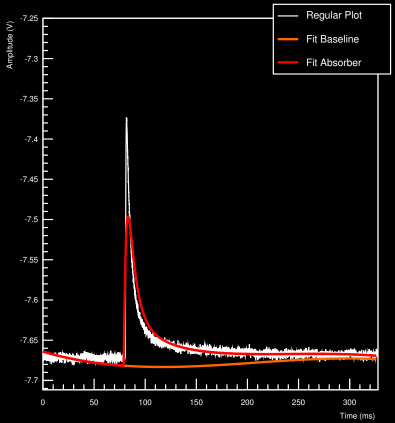

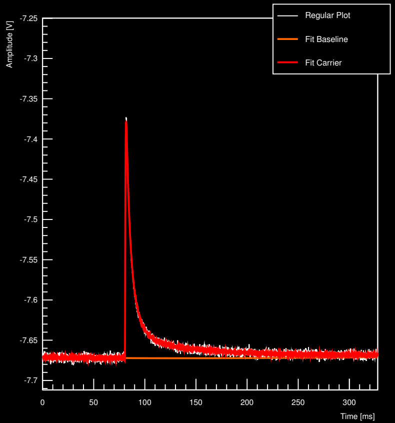

Migdal Effect

When a Dark Matter particle recoils off a target nucleus, the nucleus moves. The recoil produces a change in the electrons orbital function $\Psi \rightarrow \Psi'$.

The rearrangement of the electrons can result in different radiations produced.

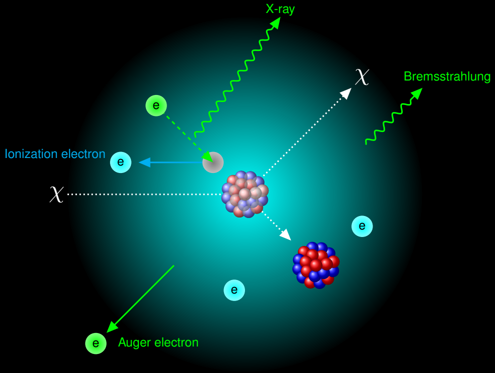

Trigger

Phase	Duration (ms)
Time window	327.68
Pre - trigger	81.92
Post - trigger	245.76
Trigger active	122.88
Trigger blocked	204.80
Readout	$\sim$2